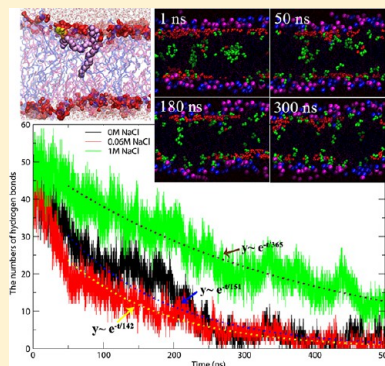


Molecular Dynamics Study of Oxidized Lipid Bilayers in NaCl Solution

Viwan Jarerattanachat,[†] Mikko Karttunen,^{*,‡} and Jirasak Wong-ekkabut^{*,†}[†]Department of Physics, Faculty of Science, Kasetsart University, 50 Phahon Yothin Rd, Chatuchak, Bangkok, Thailand[‡]Department of Chemistry and Waterloo Institute for Nanotechnology, University of Waterloo, 200 University Avenue West, Waterloo, Ontario, Canada

ABSTRACT: Polyunsaturated lipids are major targets of free radicals forming oxidized lipids through the lipid peroxidation process. Thus, oxidized lipids play a significant role in cell membrane damage. Using atomistic molecular dynamics (MD) simulations to investigate the dynamics of oxidized lipid bilayers, we examined the effects of NaCl on them. Lipid bilayer systems of 1-palmitoyl-2-linoleoyl-*sn*-glycero-3-phosphatidylcholine (PLPC) and 4 oxidation products, namely, 9-*tc*-hydroperoxide linoleic acid, 13-*tc*-hydroperoxide linoleic acid, 9-oxononanoic acid, and 12-oxo-9-didecadienoic acid in 0, 0.06, and 1 M NaCl solution were studied. These 51 systems, combined over 15 μ s of total simulation time, show Cl^- anions remaining in the water phase and Na^+ cations permeating into the headgroup region of the bilayer leading to membrane packing. The effects of NaCl on thickness and area per molecule were found to be independent of the concentration of oxidized lipids. NaCl disturbed the bilayers with aldehyde lipids more than those with peroxide lipids. The key finding is that oxidized lipids bend their polar tails toward the water interface. This behavior was monitored by following the time evolution of hydrogen bonds between the oxidized functional groups of different lipids, and the concomitant increase of hydrogen bonds between oxidized functional groups and water molecules. Our results also show that the number of hydrogen bonds should be considered as an equilibration parameter: Very long simulations are needed to equilibrate systems with high NaCl concentrations.



■ INTRODUCTION

The lipid bilayer is one of the most fundamental structures in biology. Bilayers protect cells and organelles and selectively control nutrient and waste permeation in and out of cells. The structure and permeation properties of lipid bilayers such as thickness, membrane fluidity, and permeability to different substances can be altered by lipid peroxidation.^{1,2} A direct relationship between lipid peroxidation and membrane leakiness has been suggested.^{1–4} In particular, if the bilayer consists of unsaturated fatty acids, their double bonds can react with free radicals (OH^- , O_2^+ , etc.)^{5,6} and form oxidized lipids.^{7,8}

The oxidation of phosphatidylcholines (PC) produces two major oxidized species: hydroxyl- or hydroperoxy-dieonyl PCs, and truncated chains of PCs with aldehyde or carboxylic group.⁹ Both have polar moieties at their terminals.¹⁰ Their effects are due to these structural changes. Oxidized lipids have been intensely studied for many decades because they play an important role in membrane damage and various diseases,^{11–13} including Parkinson's^{14–16} and Alzheimer's^{17–21} diseases, inflammatory response,²² atherosclerosis,^{23,24} and schizophrenia.²⁵

Lipid peroxidation critically modifies the chemical structure of PCs^{9,10} by introducing polar and hydrophilic groups into the hydrocarbon chain, i.e., inside the bilayer.^{26,27} This leads to changes in properties, for example, an increase of area per lipid and a decrease in bilayer thickness, along with a decrease in the lipids' order parameters.^{9,28,29} Some changes depend on the

type of oxidized lipids.³⁰ Such is the case with lipid lateral diffusion coefficient: Aldehyde lipids diffuse faster while peroxide lipids are slower than nonoxidized lipids.^{28,31} An increase of water penetration into bilayers containing oxidized lipids has been shown in previous studies.^{9,28,32–34} Critical membrane damage results from the reversal of the oxidized tail to water interface^{28,29,32,33} leading to water pore formation observed at high concentrations of oxidized lipids, as reported by Lis et al.³⁵ and Cwiklik et al.³⁶

Under physiological conditions, lipid bilayers are surrounded not only by water but also salt ions. Previous MD studies of oxidized lipid bilayers^{28,29,37} did not consider the effect of ions. Recent experimental studies^{38–42} have shown that monovalent cations, such as sodium, have a significant impact on lipid membranes: Ion binding enhances lipid–lipid interactions and leads to a compression of the membrane. These results are in agreement with the computational simulations focused on the effects of monovalent^{38,43–47} (NaCl and KCl) and divalent⁴³ (CaCl_2) salts on bilayers comprising zwitterionic PCs. Simulations have demonstrated that cations are able to penetrate deep into a membrane: They reach the carbonyl region and form tight complexes with lipid molecules.^{38,43–45,47} However, the character of ion binding has been suggested to be

Received: April 24, 2013

Revised: June 22, 2013

Published: June 25, 2013

Table 1. Descriptions of the 51 Lipid Bilayer Systems^a

| system | description | | | | #oxidized lipid | #PLPC | #Na ⁺ ,Cl ⁻ | time (ns) |
|--------|-------------|---|-------------|---------------|-----------------|-------|-----------------------------------|-----------|
| 1 | PLPC | | | | - | 128 | 0 | 200 |
| 2 | PLPC | + | 0.06 M NaCl | | - | 128 | 10 | 200 |
| 3 | PLPC | + | 1 M NaCl | | - | 128 | 165 | 600 |
| 4 | PLPC | + | 12-al | | 8 | 120 | 0 | 200 |
| 5 | PLPC | + | 12-al | | 16 | 112 | 0 | 200 |
| 6 | PLPC | + | 12-al | | 32 | 96 | 0 | 200 |
| 7 | PLPC | + | 12-al | | 64 | 64 | 0 | 200 |
| 8 | PLPC | + | 12-al | + 0.06 M NaCl | 8 | 120 | 10 | 400 |
| 9 | PLPC | + | 12-al | + 0.06 M NaCl | 16 | 112 | 10 | 200 |
| 10 | PLPC | + | 12-al | + 0.06 M NaCl | 32 | 96 | 10 | 200 |
| 11 | PLPC | + | 12-al | + 0.06 M NaCl | 64 | 64 | 10 | 200 |
| 12 | PLPC | + | 12-al | + 1 M NaCl | 8 | 120 | 165 | 400 |
| 13 | PLPC | + | 12-al | + 1 M NaCl | 16 | 112 | 165 | 300 |
| 14 | PLPC | + | 12-al | + 1 M NaCl | 32 | 96 | 165 | 300 |
| 15 | PLPC | + | 12-al | + 1 M NaCl | 64 | 64 | 165 | 500 |
| 16 | PLPC | + | 13-tc | | 8 | 120 | 0 | 300 |
| 17 | PLPC | + | 13-tc | | 16 | 112 | 0 | 300 |
| 18 | PLPC | + | 13-tc | | 32 | 96 | 0 | 300 |
| 19 | PLPC | + | 13-tc | | 64 | 64 | 0 | 700 |
| 20 | PLPC | + | 13-tc | + 0.06 M NaCl | 8 | 120 | 10 | 200 |
| 21 | PLPC | + | 13-tc | + 0.06 M NaCl | 16 | 112 | 10 | 200 |
| 22 | PLPC | + | 13-tc | + 0.06 M NaCl | 32 | 96 | 10 | 200 |
| 23 | PLPC | + | 13-tc | + 0.06 M NaCl | 64 | 64 | 10 | 500 |
| 24 | PLPC | + | 13-tc | + 1 M NaCl | 8 | 120 | 165 | 500 |
| 25 | PLPC | + | 13-tc | + 1 M NaCl | 16 | 112 | 165 | 300 |
| 26 | PLPC | + | 13-tc | + 1 M NaCl | 32 | 96 | 165 | 500 |
| 27 | PLPC | + | 13-tc | + 1 M NaCl | 64 | 64 | 165 | 500 |
| 28 | PLPC | + | 9-al | | 8 | 120 | 0 | 200 |
| 29 | PLPC | + | 9-al | | 16 | 112 | 0 | 200 |
| 30 | PLPC | + | 9-al | | 32 | 96 | 0 | 200 |
| 31 | PLPC | + | 9-al | | 64 | 64 | 0 | 200 |
| 32 | PLPC | + | 9-al | + 0.06 M NaCl | 8 | 120 | 10 | 200 |
| 33 | PLPC | + | 9-al | + 0.06 M NaCl | 16 | 112 | 10 | 200 |
| 34 | PLPC | + | 9-al | + 0.06 M NaCl | 32 | 96 | 10 | 200 |
| 35 | PLPC | + | 9-al | + 0.06 M NaCl | 64 | 64 | 10 | 200 |
| 36 | PLPC | + | 9-al | + 1 M NaCl | 8 | 120 | 165 | 400 |
| 37 | PLPC | + | 9-al | + 1 M NaCl | 16 | 112 | 165 | 450 |
| 38 | PLPC | + | 9-al | + 1 M NaCl | 32 | 96 | 165 | 400 |
| 39 | PLPC | + | 9-al | + 1 M NaCl | 64 | 64 | 165 | 400 |
| 40 | PLPC | + | 9-tc | | 8 | 120 | 0 | 200 |
| 41 | PLPC | + | 9-tc | | 16 | 112 | 0 | 200 |
| 42 | PLPC | + | 9-tc | | 32 | 96 | 0 | 200 |
| 43 | PLPC | + | 9-tc | | 64 | 64 | 0 | 200 |
| 44 | PLPC | + | 9-tc | + 0.06 M NaCl | 8 | 120 | 10 | 200 |
| 45 | PLPC | + | 9-tc | + 0.06 M NaCl | 16 | 112 | 10 | 200 |
| 46 | PLPC | + | 9-tc | + 0.06 M NaCl | 32 | 96 | 10 | 200 |
| 47 | PLPC | + | 9-tc | + 0.06 M NaCl | 64 | 64 | 10 | 200 |
| 48 | PLPC | + | 9-tc | + 1 M NaCl | 8 | 120 | 165 | 400 |
| 49 | PLPC | + | 9-tc | + 1 M NaCl | 16 | 112 | 165 | 400 |
| 50 | PLPC | + | 9-tc | + 1 M NaCl | 32 | 96 | 165 | 400 |
| 51 | PLPC | + | 9-tc | + 1 M NaCl | 64 | 64 | 165 | 400 |

^aTotal simulation time: 15.25 μ s.

sensitive, at least to some degree, upon force-field parametrization.^{47–52}

Independent of the force-field, characteristic times for ion binding to the bilayer were found to be long, at least 30 ns for sodium ions and 100 ns for divalent calcium ions.^{43,47} The residence time distributions of cations (Na⁺) and anions (Cl⁻) were found to be different:⁴⁷ For Cl⁻, an exponential decay was

reported but the Na⁺ resident time appeared to follow a power law explaining the observed long resident times.⁴⁷ The binding of cations has a significant impact on the structural and dynamical properties of PC membranes.^{45,48} A decrease of area per lipid and lipid lateral diffusion coefficient as an increase of salt concentration had been shown in MD simulations^{45,48,53} in agreement with the decrease of the angle between the P–N

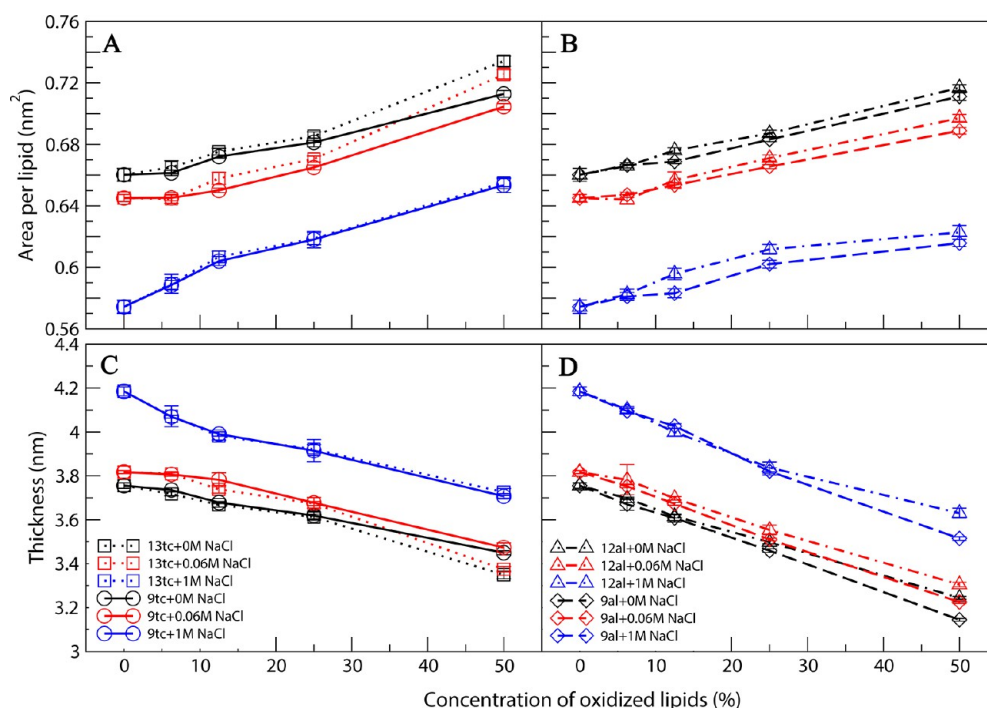


Figure 1. Area per molecule (A and B) and thickness (C and D) for PLPC bilayers containing oxidized lipids at concentrations ranging from 0% to 50%. NaCl solutions of 0, 0.06, and 1 M were used.

vector of the lipid head and bilayer normal⁴⁵ and the increase of lipid tail order.^{38,44} However, the experiments done by Ferber et al.⁵⁴ did not find a significant change in area per lipid, though tilting of the lipids' head groups out of the membrane plane was noted.

We study the effect of monovalent salt on bilayers containing oxidized lipids. Oxidized lipids greatly disturb the lipid bilayer from inside the bilayer—lipid tails with polar group bend toward the water interface—and the monovalent cations penetrate deep from water into headgroup region. We investigate their interactions and the effect on the structure and dynamics of lipids, ion binding, and hydrogen bonding. We performed atomistic MD simulations of 1-palmitoyl-2-linoleoyl-*sn*-glycero-3-phosphatidylcholine (PLPC) lipid bilayers with the various concentrations of 4 PLPC's oxidation products²⁸ (details in the next section) in 0, 0.06, and 1 M NaCl solutions.

MOLECULAR DYNAMICS SIMULATION

We performed MD simulations of bilayers composed of a total of 128 lipid molecules. 1-Palmitoyl-2-linoleoyl-*sn*-glycero-3-phosphatidylcholine (PLPC) lipids were used to model an unsaturated lipid bilayer. Bilayers were constructed with four of the major oxidative products of linoleic acid,^{7,8,55} including either a hydroperoxide or an aldehyde group: 9-*trans*,*cis*-hydroperoxide linoleic acid (9-*tc*), 13-*trans*,*cis*-hydroperoxide linoleic acid (13-*tc*), 9-oxo-nonanoic acid (9-*al*), and 12-oxo-9-dodecenoic acid (12-*al*). These oxidized chains replaced the *sn*-2 linoleate chains in PLPCs.²⁸ Mixtures of oxidative lipid bilayers were prepared by replacing 8, 16, 32, or 64 PLPC lipids with oxidized ones. They correspond to 6.25%, 12.5%, 25%, and 50% molar concentrations, respectively. The force-field for oxidized lipids has been described and tested before.²⁸ The lipid bilayers were fully hydrated by a single point charge (SPC) water molecules.⁵⁶ NaCl^{49,57} was added at concentrations of 0

M, 0.06 M, and 1 M. The simulation box size was about $(6.6 \times 6.7 \times 6.1)$ nm³.

The numbers of molecules are shown in Table 1. A total of 51 simulations were run with GROMACS version 4.⁵⁸ After energy minimization, each MD simulation ran for at least 200 ns with an integration time step of 2 fs. The initial 100 ns (in some cases more as will be discussed later) were considered as an equilibration period by monitoring the area per lipid, and bilayer thickness. The total simulation time was 15.25 μ s. Periodic boundary conditions were applied in all dimensions. A 1.0 nm cutoff was employed for the real-space part of electrostatic and Lennard-Jones interactions. The long-range electrostatics was calculated using particle-mesh Ewald^{59–61} with the reciprocal-space interactions evaluated on a 0.12 nm grid with cubic interpolation of order four. The neighbor list was updated at every time step.⁶² The above protocol was employed to avoid physical artifacts.^{62–64} The LINCS algorithm was used to constrain all bond lengths.⁶⁵ The weak temperature coupling scheme was applied separately to the lipids and water (ions were grouped with water molecules)⁶⁶ with a temperature of 298 K and a time constant of 0.1 ps. Semi-isotropic pressure was applied,⁶⁶ with an equilibrium pressure of 1 bar both in the *x*–*y* plane and in the *z*-direction (bilayer normal) with a time constant of 3.0 ps and a compressibility of 4.5×10^{-5} bar⁻¹. Molecular visualizations were done using Visual Molecular Dynamics (VMD) software.⁶⁷

RESULTS AND DISCUSSION

Effect of Oxidized Lipids on Bilayer Dimensions. The area per lipid increased when the number of oxidized lipids was increased. This was accompanied by a decrease in thickness, shown in Figure 1. This is consistent with previous computational and experimental studies.^{28,68} However, the difference in values especially at low concentration of oxidized lipids is

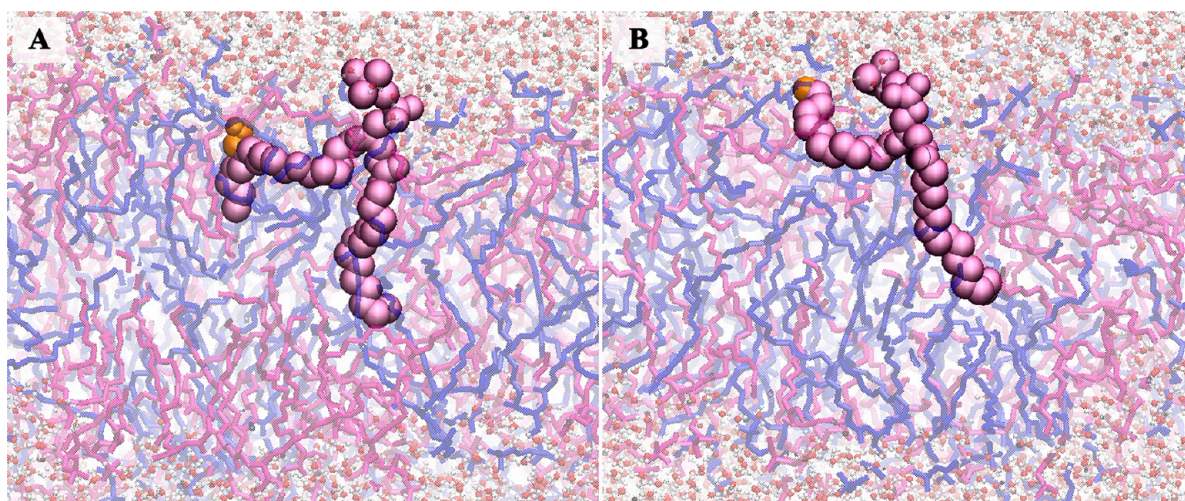


Figure 2. Snapshots of 13tc (A) and 12al (B) lipids in lipid bilayers. Oxidized lipids bend their polar tails toward the water interface. Orange color shows the functional group.

simply due to the fact that the simulations presented in this manuscript are for larger (more representative) systems, several times longer than those in ref 28, and thus better equilibrated. The bilayer, with 50% of oxidized lipids, showed the largest changes. Oxidized lipids disturbed the bilayer by bending their polar tails toward the water interface (as shown in Figure 2). This implies that changes in bilayer dimensions are closely related to the type of functional groups in oxidative lipids. The bilayers containing peroxide lipids (13tc and 9tc) showed similar values of thickness and area per molecule. Compared to the bilayers containing aldehyde lipids, the bilayers with peroxide lipids had larger areas per molecule and smaller thickness.

Effect of NaCl on Oxidized Lipid Bilayers. NaCl solutions of 0, 0.06, and 1 M were used (Table 1). For all lipid bilayers, we found that the bilayer thickness increased and the area per molecule decreased when the NaCl concentration increased. The presence of monovalent cations lead to membrane compression similar to what has been previously demonstrated for other lipids.^{38,44,45,47,48,69,70} In this manuscript, the distance between the phosphate atoms of the two monolayers is used as a definition of the bilayer's thickness. For the pure PLPC bilayers, we found the average thicknesses of 3.76 ± 0.01 nm (0 M NaCl), 3.82 ± 0.01 nm (0.06 M NaCl), and 4.18 ± 0.02 nm (1 M NaCl) and areas per lipid of 0.660 ± 0.004 nm² (0 M NaCl), 0.645 ± 0.002 nm² (0.06 M NaCl), and 0.574 ± 0.004 nm² (1 M NaCl). The bilayers, with oxidized lipids at various NaCl concentrations, showed qualitative behavior similar to the pure PLPC as seen in Figures 1 and 3. The changes in thickness and area per molecule are similar for all lipid compositions (Figures 1): The thickness increases by $\sim 2\%$ (0.06 M NaCl) and $\sim 10\%$ (1 M NaCl), as compared to the system without NaCl. The area per molecule decreased by $\sim 2\%$ and $\sim 11\%$ in 0.06 and 1 M NaCl solutions, respectively.

NaCl disturbs the aldehyde (9al and 12al) lipid bilayers slightly more than the peroxide (9tc and 13tc) ones at low NaCl concentration (0.06 M). The perturbations become significant at higher NaCl concentration (1 M): The thickness and the area per molecule of the systems with aldehyde lipids changed by $\sim 11\%$ and $\sim 12\%$, respectively, when 1 M NaCl is added. Meanwhile, the bilayers containing peroxide lipids

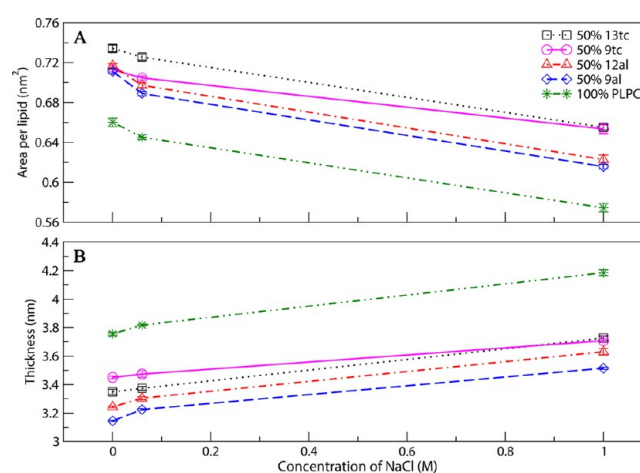


Figure 3. Area per molecule (A) and thickness (B) of oxidized lipid bilayers solvated in 0, 0.06, and 1 M NaCl solutions. The legend shows the type of oxidized lipid. In all cases 50% of the lipids were oxidized (with the exception of pure PLPC).

experienced slightly smaller changes, $\sim 9\%$ in thickness and $\sim 10\%$ in the area per molecule. The effects of NaCl on thickness and area per molecule of bilayers with oxidized bilayers were found to be independent of the concentration of oxidized lipids. The particular structure of an oxidized lipid is, however, a factor. A previous systematic study of pure DPPC bilayers at various concentrations of NaCl solutions showed that cations bind to the headgroup region of a membrane, while chloride anions mostly stay in the water phase, leading to notable membrane compression.^{47,71}

Order Parameter. The changes in membrane thickness and area are related to the ordering of lipid chains.⁷² The salt-induced changes can be determined by the deuterium order parameter (S_{CD}). S_{CD} can be experimentally measured by using NMR⁷³ and it is defined as

$$S_{CD} = \frac{1}{2} \langle 3 \cos^2(\theta) - 1 \rangle \quad (1)$$

where θ is the angle between a C–D bond and the membrane normal. The brackets indicate averaging over all the lipids and over time. Since a united-atom representation was used in our

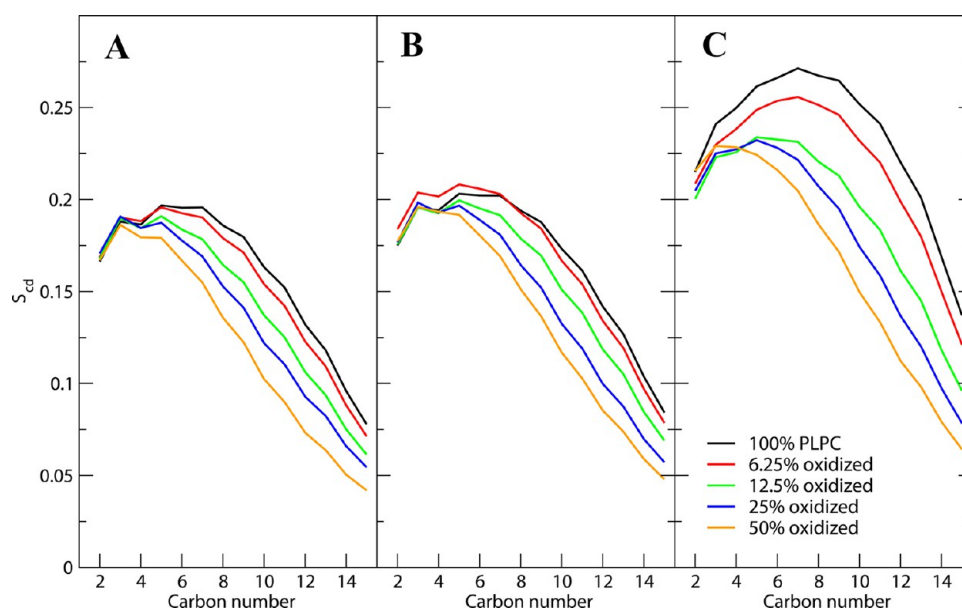


Figure 4. Deuterium order parameter of PLPC's sn-1 tail in the presence of different concentrations of 12al oxidized lipids. NaCl concentrations: 0 (A), 0.06 (B), and 1 (C) M.

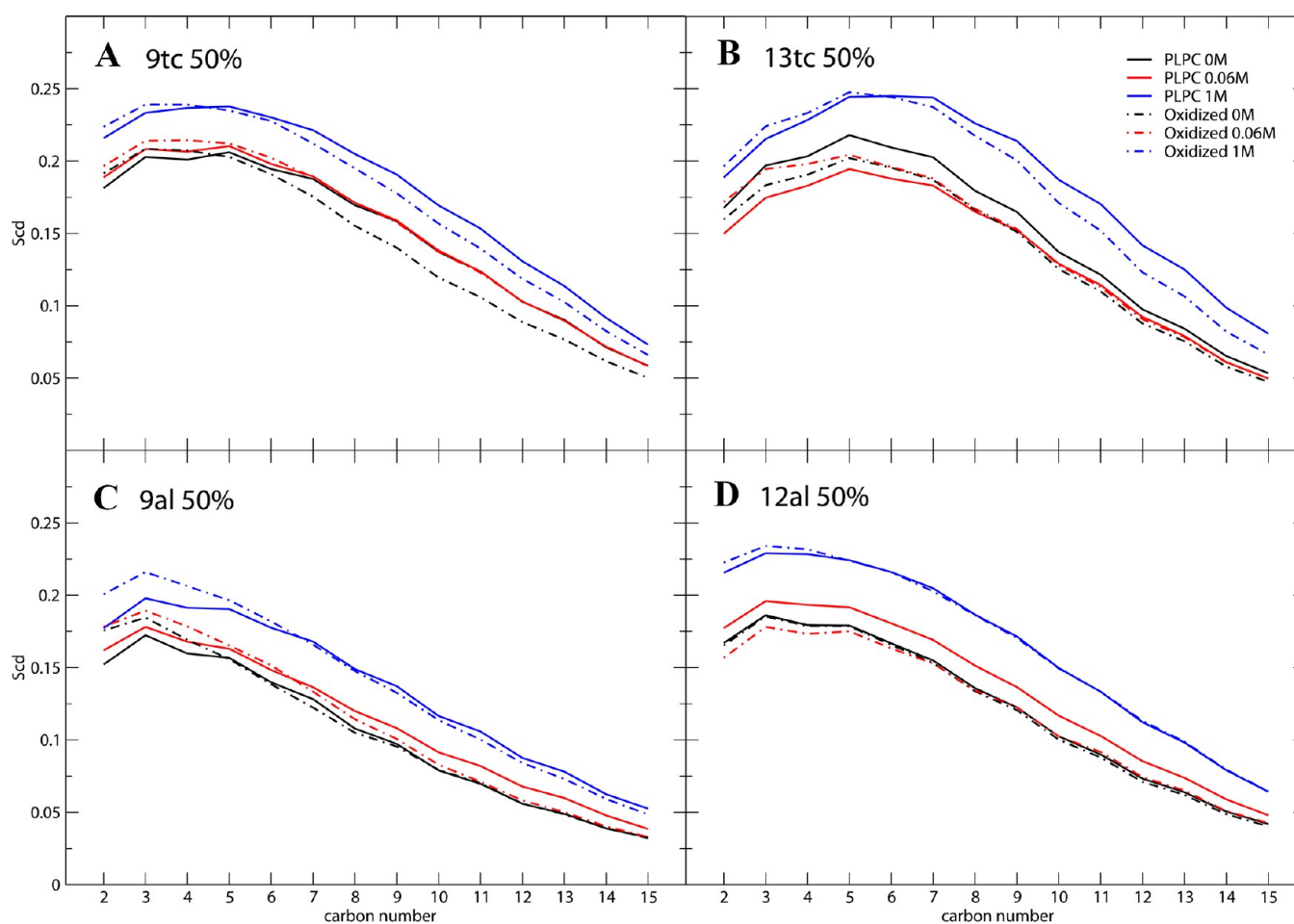


Figure 5. Deuterium order parameters of PLPC sn-1 tails and oxidized lipids in 0, 0.06, and 1 M NaCl concentrations. 50% of the lipids are oxidized.

simulations, the positions of the deuterium atoms were reconstructed assuming ideal tetrahedral geometry of the methylene groups.⁷⁴ A comparison of S_{CD} (PLPC sn-1 tail) shows that order decreases with an increasing concentration of

oxidized lipids. The PLPC sn-1 tail in the 50% oxidized lipid mixture shows significant disorder compared to the pure lipid bilayer especially for the carbon atoms deeper in the bilayer (Figure 4). In the presence of NaCl, lipid tails gain a

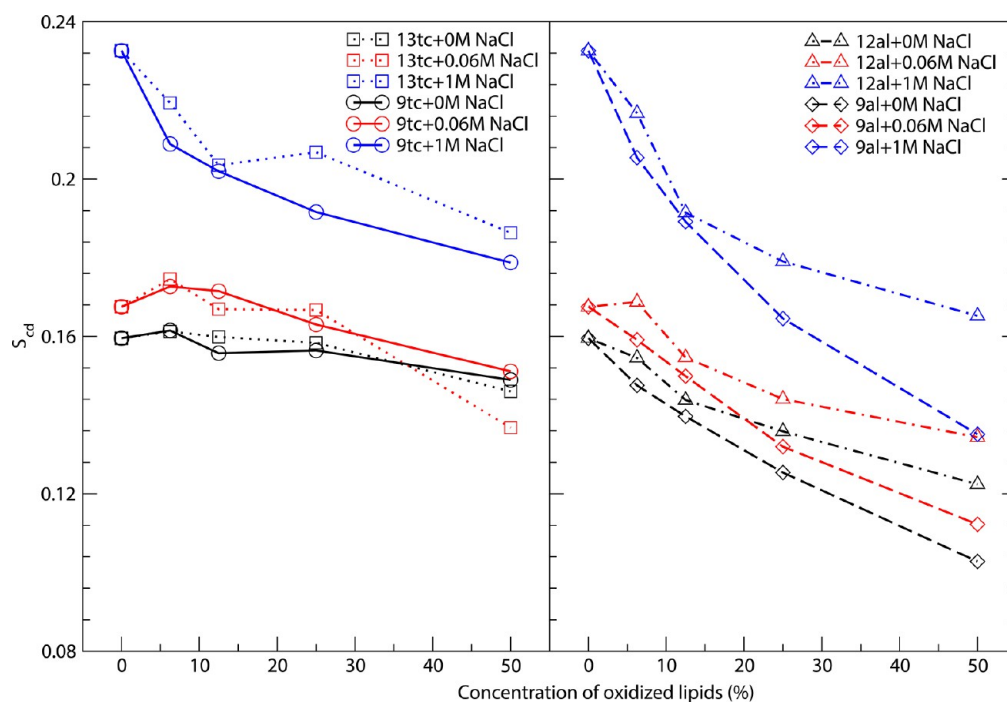


Figure 6. Average deuterium order parameter (averaged over all carbon atoms in the lipid hydrocarbon chain) of PLPC's sn-1 chain as a function of oxidized lipid concentration.

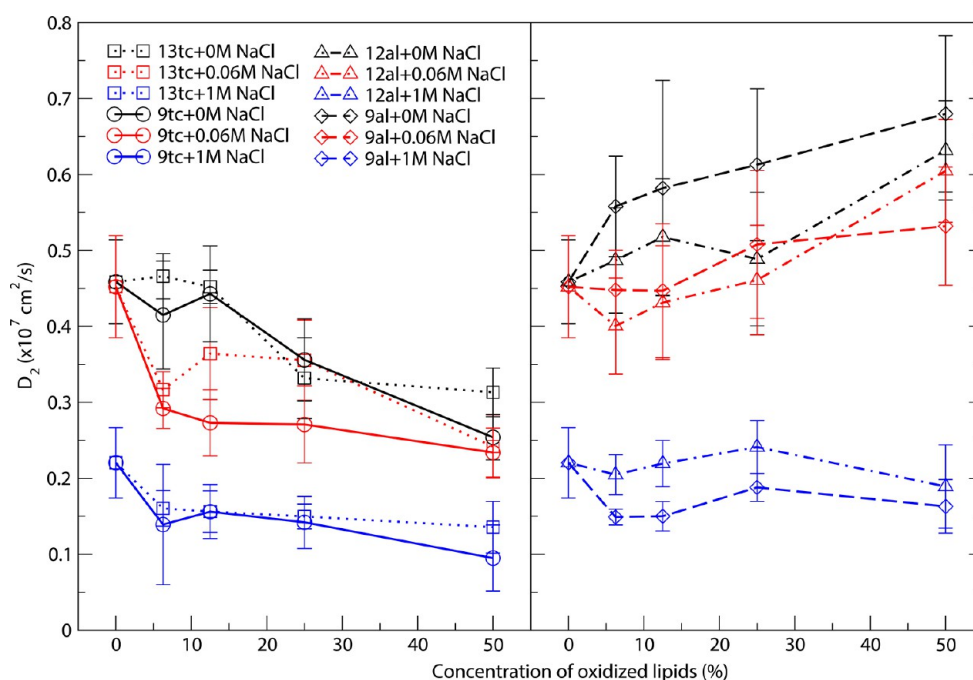


Figure 7. Average long time (D_2) lateral diffusion coefficients of lipid molecules as a function of oxidized lipid concentration at NaCl concentrations of 0, 0.06, and 1 M.

significantly higher order than without NaCl as shown in Figure 5. This finding is in agreement with previous studies on different systems.^{38,44,45,75} The bilayers in 1 M NaCl solution have a significantly higher order parameter than those in 0 and 0.06 M NaCl, and the order parameter decreases with increasing concentration of oxidized lipids (Figure 6). The effect of NaCl tends to depend on the position of the functional group along the lipid tail: The bilayers with 9tc and 9al are less

ordered than the ones with 13tc and 12al (Figure 6). This effect is enhanced at 1 M NaCl solution as shown in Figure 6.

Lateral Diffusion. To estimate the lateral diffusion coefficient of lipid molecules, we divided the trajectories into 50 ns windows. The mean square displacements (MSD) were calculated relative to their monolayer's center of mass as a function of time. Then, the data between 0 and 20 ns were fitted to^{47,76}

$$\langle r^2 \rangle = \frac{4D_1 t r_0^2}{r_0^2 + 4D_1 t} + 4D_2 t \quad \text{where} \quad r_0^2 \equiv \frac{R}{2} \quad (2)$$

Diffusion occurs at different time scales,⁷⁷ and here we characterize diffusion by short-time (D_1) and long-time (D_2) diffusion coefficients. The former corresponds to ballistic or near-ballistic motion. D_1 can be measured by neutron scattering experiments^{78–80} on picosecond time scale. The values of D_1 have been reported in the range of $(1–10) \times 10^{-7} \text{ cm}^2/\text{s}$.^{78,79} D_2 can be measured by, for example, fluorescence correlation spectroscopy (FCS) on millisecond time scales which typically give values around $(0.5–1) \times 10^{-7} \text{ cm}^2/\text{s}$. This corresponds to Brownian motion.^{28,38,81,82}

If both the oxidized lipid and NaCl concentrations are varied, results show that the short time diffusion coefficients (D_1) are not significantly different from each other. This is in agreement with the view first provided by Falck et al.⁸¹ and experimentally confirmed by Busch et al.⁸⁰ The average value of D_1 for all systems is approximately $(7.42 \pm 0.78) \times 10^{-7} \text{ cm}^2/\text{s}$. This value is lower than D_1 for DMPC ($13 \times 10^{-7} \text{ cm}^2/\text{s}$)⁷⁶ and PLPC ($(10.4 \pm 0.4) \times 10^{-7} \text{ cm}^2/\text{s}$) lipid with previous reports,²⁸ but the previous reports were obtained in the system without NaCl. When long-time diffusion (D_2) is taken into consideration, the differences between D_2 under various oxidized lipid concentration at the same concentration of NaCl are within the margin of error from each other.²⁸ However, a qualitative trend can be observed for different types of oxidized lipids. When the concentration of oxidized lipids is increased, D_2 of the aldehyde lipid mixture increases. A similar trend was shown in the cationic lipid mixture.⁴⁷ Peroxide lipids show the opposite behavior because of the heavier molecules and strong interaction between their functional groups, shown in Figure 7. However, at 1 M of NaCl, all the systems behave very similarly without any noticeable differences. Figure 8

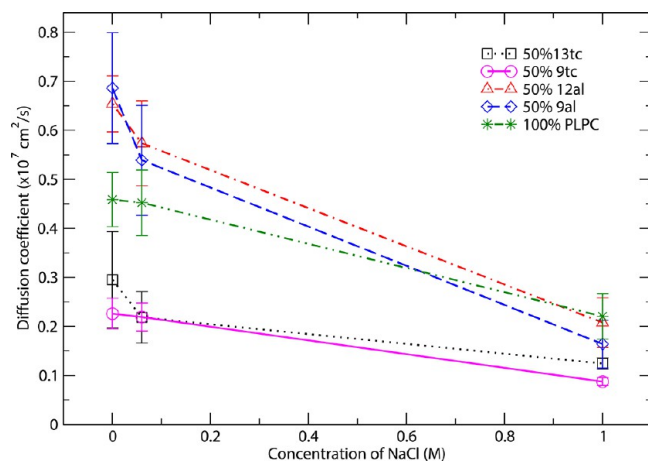


Figure 8. Average long time (D_2) lateral diffusion coefficients of lipid molecules in 50% oxidized lipid mixture bilayer as a function of NaCl concentration.

shows the effect of NaCl concentration on the diffusion coefficient D_2 . The lipids are significantly slowed down when the concentration of ions increases. The reduction in lipid diffusion coefficient could be explained by formation of complexes of Na^+ ions with lipids.^{38,47} This is in agreement with the decrease in the area per molecule and the higher degree of ordering of the sn-1 chain in the presence of Na^+ in bilayer.

Hydrogen Bonding (HB) of Functional Groups. The number of hydrogen bonds between the functional groups of oxidized lipids and water molecules was calculated with the usual geometric definition: A hydrogen bond was defined to exist if the distance between the donor and the acceptor was $r_{\text{HB}} < 0.35 \text{ nm}$ and the angle $\alpha_{\text{OH}} < 30^\circ$. The value of 0.35 nm corresponds to the first minimum of the radial distribution function (RDF) of water. Figure 9 shows the numbers of hydrogen bonds between the functional groups of the oxidized lipids and water molecules as a function of time. The different initial values are simply a reflection of the different starting configurations, and the evolution toward equilibrium (and, as it turns out, toward the same H-bond numbers) is clear from the figure. The time for the hydrogen bond population to reach equilibrium depends upon both the concentration of NaCl and the functional group of the oxidized lipid. The higher the NaCl concentration, the longer equilibration took. The peroxide lipid mixture reached equilibrium more slowly than the aldehyde lipid mixture. At 1 M NaCl, the aldehyde lipid mixture reached equilibrium after approximately 100 ns. Figure 10 shows the number of hydrogen bonds between the peroxide groups of different oxidized lipids for 50% 13tc mixtures bilayers with 0, 0.06, and 1 M. The figure shows an exponential decrease as a function of time with characteristic time scales of 151, 142, and 365 ns, respectively. The long times are due to the interactions of ions with the oxidative functional groups. This slowly evolving property should be monitored to identify the necessary equilibration period. Although these times are very long, they do not seem to have influence on properties such as area per lipid.

Two oxygen atoms in the peroxide group provide strong interactions with the water molecules: It is easier for the tails of the peroxide lipids to form hydrogen bonds and bend their tails toward the lipid–water interface, Figure 11. Aldehyde lipids behaved qualitatively the same way, but hydrogen bonding was weaker due to only single oxygen in the functional group. Thus, characteristic times were shorter.

To determine the tilt angle distribution of the oxidized lipid tails (Figure 12), the angles between the vector from the first carbon to the oxidized carbon and the bilayer normal were calculated. The results show that the dominant peaks of all oxidized lipid species are in the range of $96–118^\circ$, implying that most oxidized tails prefer to bend their functional group toward the water interface. Therefore, the shape of distribution depends on the position of the functional group in the lipid tail and NaCl concentration. Broader distributions occur in the systems of 13tc and 12al, where the oxidized functional group is located deeper in the bilayer than in the systems of 9tc and 9al. The second peak corresponds to an additional preferred position of the oxidized functional group. For 12al with 1 M NaCl, the second peak appears approximately at 156° . This implies that the aldehyde group stays in the bilayer, as rather two differently oriented populations of aldehyde seem to be present. Additional analysis of the contacts between the aldehyde groups of the different leaflets (Figure 13) showed that the features in Figure 12 (appearance of the shoulder and the second peak) are stable.

To study the interactions of cations with the lipid head groups, the averaged cation–lipid coordination numbers were calculated following Gurtovenko et al. and Lee et al.,^{45,69} Figure 14. All oxygen atoms in the lipid head groups, including the ones in phosphate and carbonyl groups, were used as the lipid headgroup representation. The cutoff distance between a cation

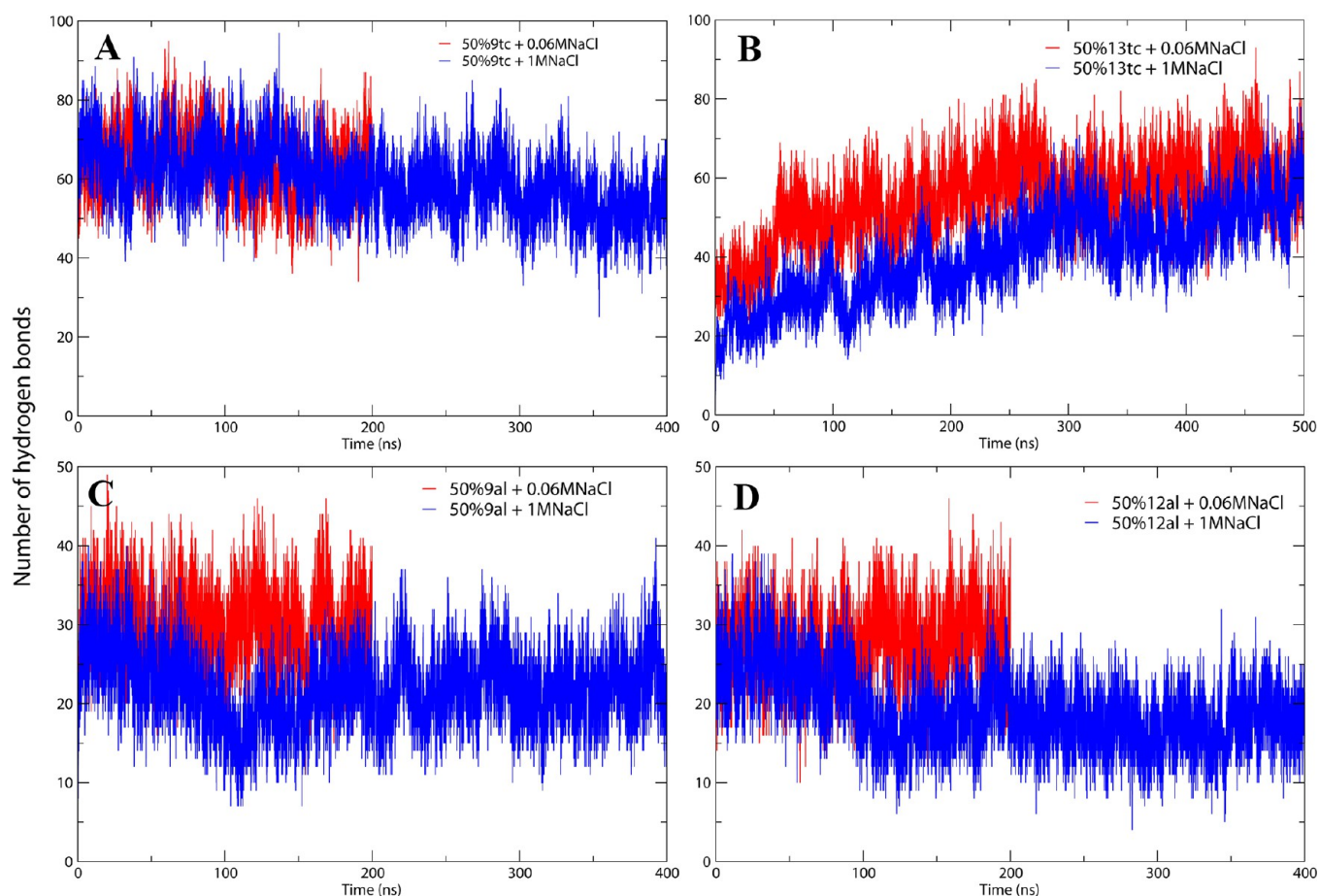


Figure 9. Number of hydrogen bonds between oxidized lipids and water molecules as a function of time.

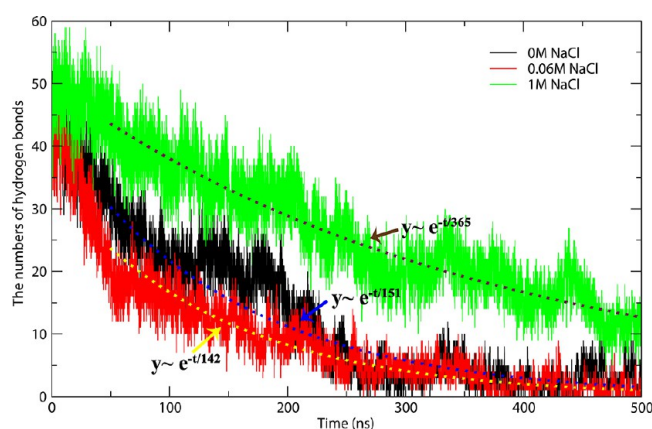


Figure 10. The number of hydrogen bonds between peroxide groups in 50% 13tc mixture bilayers solvated at 0 (black), 0.06 (red) and 1 M (green) NaCl solution as a function of time. The number of hydrogen bonds decreases exponentially with the characteristic times of 151 (0M), 142 (0.06M) and 365 (1M) ns.

and an oxygen in a lipid headgroup was determined from the first minimum of the corresponding radial distribution function. The cutoff distances were 0.328 and 0.334 nm for 0.06 and 1 M NaCl solutions, respectively. At low salt concentration (0.06 M NaCl), all Na^+ ions entered the bilayer. The bilayers with oxidized lipids (the averaged value of all oxidized systems is 4.21 ± 0.44) had higher coordination numbers for Na^+ with the lipid head than the pure bilayers (the value is 3.57 ± 0.14).

There was no difference in coordination numbers for the different functional groups: The average coordination numbers of the peroxide and aldehyde lipid bilayers were 4.20 ± 0.06 and 4.21 ± 0.05 , respectively. The larger fluctuations for the case of low salt concentrations are due to the fairly low absolute number of ions (this is unavoidable due to system size limitations for MD simulations). For the 1 M NaCl solution, the coordination numbers of all bilayers become very similar and their average value decreased to 1.81 ± 0.16 . This reduction is due to the saturation of Na^+ in bilayer and the electrostatic repulsion.

CONCLUSIONS

The effects of NaCl on oxidized lipid bilayers were studied using MD simulations. The results show that sodium ions permeate into the bilayer headgroup region leading to membrane packing. NaCl has a stronger effect on the aldehyde lipids than on peroxide lipids. This is manifested in bilayer thickness, area per lipid, and the number of hydrogen bonds between the functional groups and water. The bilayer with aldehyde lipids at 1 M NaCl undergoes $\sim 11\%$ increase in thickness and $\sim 12\%$ decrease in area per lipid. The changes in the bilayer with peroxide lipids are slightly smaller, $\sim 9\%$ increase in thickness and $\sim 10\%$ decrease in area per lipid. Considering the numbers of hydrogen bonds formed by the functional groups of the oxidized lipids with the other components of the systems, the peroxide mixture bilayers have significantly longer equilibration times than the aldehyde mixture bilayers especially in 1 M NaCl solution. We suggest

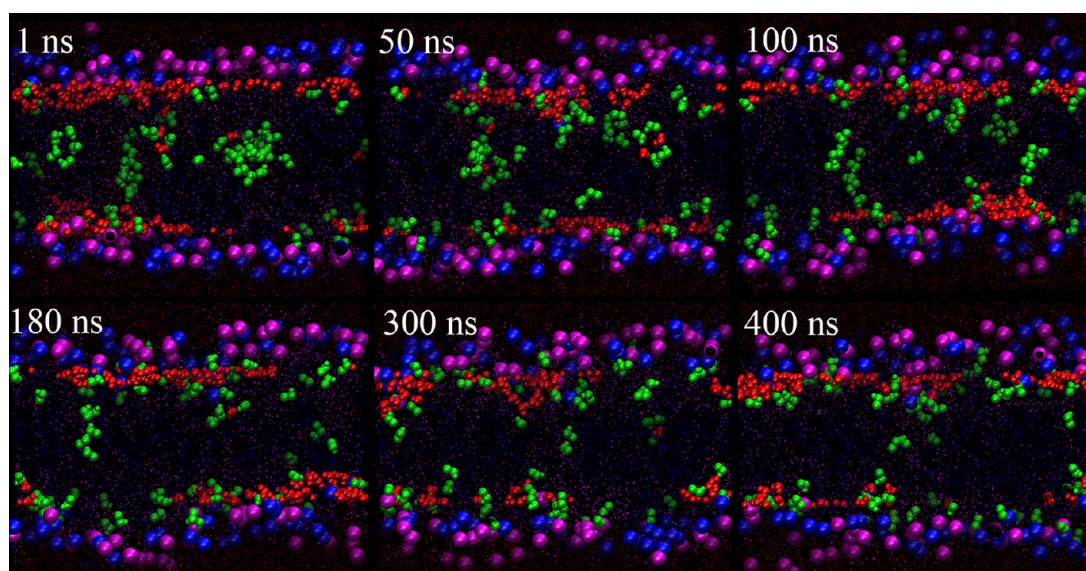


Figure 11. Snapshots of 50% 13tc bilayers at 0.06 M NaCl solution at 1, 50, 100, 180, 300, and 400 ns. The blue and purple spheres represent the phosphates of PLPC and 13tc lipids, respectively. The red spheres show the water molecules which reside inside the membrane. The green spheres display the peroxide groups (-OOH) at the ends of the 13tc lipids' tails. At 0 ns, most of the peroxide groups are inside bilayer. They move gradually toward the lipid–water interface.

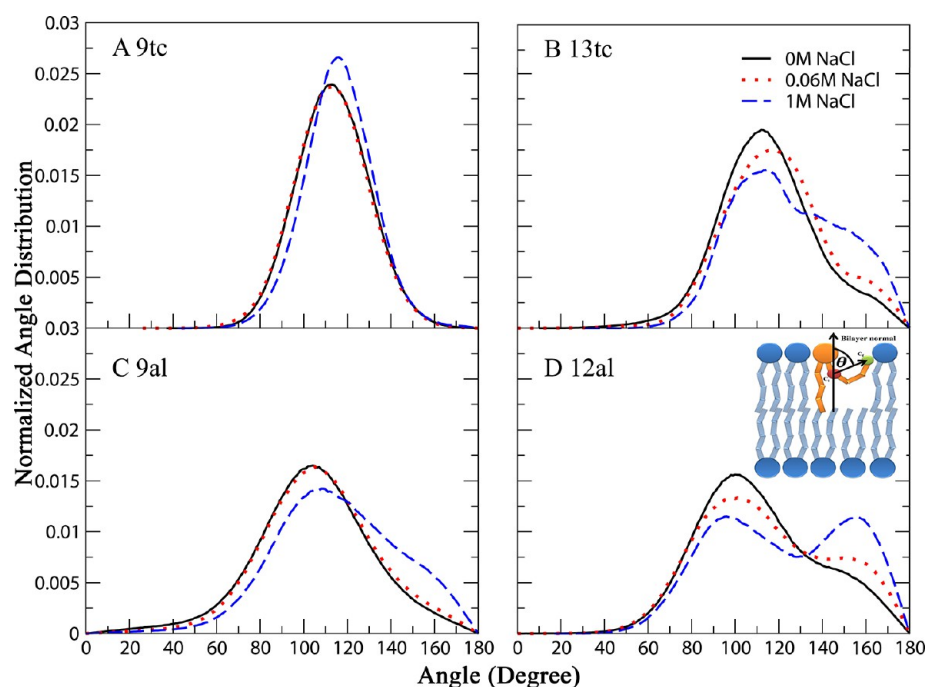


Figure 12. Tilt angle distributions for the oxidized lipid tails: 9tc(A), 13tc(B), 9al(C), and 12al(D). 50% of the lipids in bilayer are oxidized. The legend shows the salt concentrations. The angle between the vector from the first carbon to the oxidized carbon and bilayer normal was used. The inset in (D) shows the definition of the tilt angle.

that the time evolution of the number of hydrogen bonds should be considered as an equilibrium parameter. Over 300 ns was required at high NaCl concentrations. Some systems, such as 50% 13tc, appear to need more than 500 ns. Order parameter measurements show that tail order increases dramatically when NaCl is added and the change depends upon the position of functional group in lipid tail: Bilayers with 9tc and 9al are less ordered than 13tc and 12al. One of the most interesting observations was that, in lipid tail tilt angle distribution, a second peak emerged in the case of 12al: The

primary peak was at approximately around 96–118° corresponding to a tail that has tilted almost parallel to the membrane plane (see, e.g., Figures 2B and 12). The second peak at around 156° is, however, along the direction of the bilayer normal. The emergence of two such different conformations may allow for the lipids to interact through their functional groups. One may even speculate that such flexibility in orientation may provide a pathway to pore formation at longer time scales since bending of the chain exposes some of the bilayer interior to ions and water. Whether

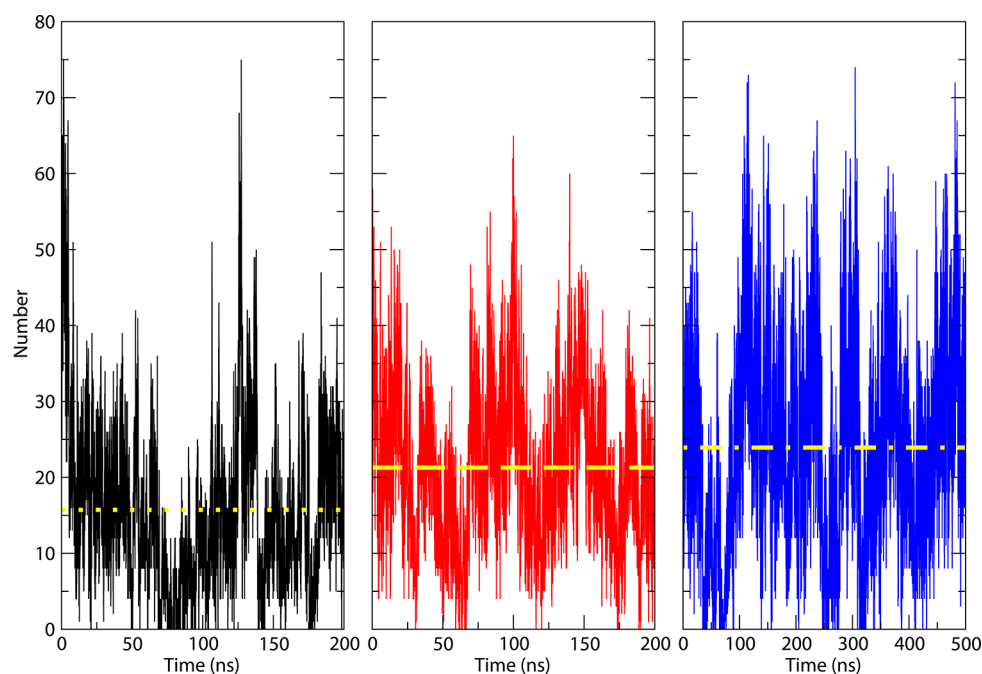


Figure 13. Numbers of contacts between the aldehyde groups of the different leaflets. The bilayers were oxidized by 50% of 12al lipids. The averaged contacts of aldehyde bilayers solvated in 0 (black line), 0.06 (red line), and 1 (blue line) M of NaCl solutions are 15.7 ± 2.4 (dotted line), 21.3 ± 1.6 (dashed line), and 23.9 ± 1.2 (dot-dashed line), respectively. The cutoff distance between two aldehyde groups is 0.6 nm, where the value is determined from the first minimum RDF of oxygen atoms.

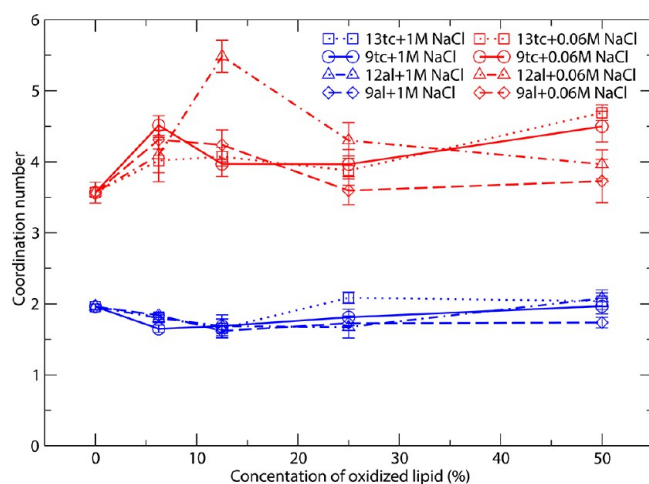


Figure 14. Coordination number of Na^+ ion and oxygen atoms in lipid's headgroup as a function of the oxidized lipid concentration. The bilayers were solvated in 0.06 (red) and 1 (blue) M NaCl concentrations.

or not that happens is beyond the scope of this study, however. This change in the distribution appears to depend on the position of the functional group along the chain and salt concentration. Finally, the long time diffusion coefficient (D_2) of the lipids decreased as NaCl concentration increased. At 1 M NaCl concentration, D_2 values for all the systems were the same (within error bars).

AUTHOR INFORMATION

Corresponding Author

*J.W.: Phone +66-2562-5555 ext 3047; E-mail jirasak.w@ku.ac.th. M.K.: Phone +1-519-888-4567 ext. 31390; E-mail mikko.karttunen@uwaterloo.ca.

Notes

The authors declare no competing financial interest.

ACKNOWLEDGMENTS

Financial support was provided by the Thailand Research Fund (TRF) [JW], the Commission on Higher Education (CHE), Ministry of Education [JW], Kasetsart University Research and Development Institute (KURDI) [JW], Faculty of Science at Kasetsart University [JW], the Graduate School at Kasetsart University [JW], the Natural Sciences and Engineering Research Council of Canada [MK], and University of Waterloo [MK]. Computational resources were provided by SHARC-NET (www.sharcnet.ca), Compute Canada and the Department of Physics, Faculty of Science, Kasetsart University.

REFERENCES

- (1) Mandal, T. K.; Chatterjee, S. N. Ultraviolet- and sunlight-induced lipid peroxidation in liposomal membrane. *Radiat. Res.* **1980**, *83*, 290–302.
- (2) Chatterjee, S. N.; Agarwal, S. Liposomes as membrane model for study of lipid peroxidation. *Free Radic. Biol. Med.* **1988**, *4*, 51–72.
- (3) Kunimoto, M.; Inoue, K.; Nojima, S. Effect of ferrous ion and ascorbate-induced lipid peroxidation on liposomal membranes. *Biochim. Biophys. Acta Biomembr.* **1981**, *646*, 169–178.
- (4) Nakazawa, T.; Nagatsuka, S.; Yukawa, O. Effects of membrane stabilizing agents and radiation on liposomal membranes. *Drugs Exp. Clin. Res.* **1986**, *12*, 831–835.
- (5) Brodnitz, M. H.; Nawar, W. W.; Fagerson, I. S. Autoxidation of saturated fatty acids. I. The initial products of autoxidation of methyl palmitate. *Lipids* **1968**, *3*, 59–64.
- (6) Brodnitz, M. H.; Nawar, W. W.; Fagerson, I. S. Autoxidation of saturated fatty acids. II. The determination of the site of hydroperoxide groups in autoxidizing methyl palmitate. *Lipids* **1968**, *3*, 65–71.
- (7) Spittler, P.; Kern, W.; Reiner, J.; Spittler, G. Aldehydic lipid peroxidation products derived from linoleic acid. *Biochim. Biophys. Acta* **2001**, *1531*, 188–208.

- (8) Pratt, D. A.; Mills, J. H.; Porter, N. A. Theoretical calculations of carbon-oxygen bond dissociation enthalpies of peroxy radicals formed in the autoxidation of lipids. *J. Am. Chem. Soc.* **2003**, *125*, 5801–5810.
- (9) Jurkiewicz, P.; Olzyska, A.; Cwiklik, L.; Conte, E.; Jungwirth, P.; Megli, F. M.; Hof, M. Biophysics of lipid bilayers containing oxidatively modified phospholipids: Insights from fluorescence and EPR experiments and from MD simulations. *Biochim. Biophys. Acta* **2012**, *1818*, 2388–2402.
- (10) Fruhwirth, G. O.; Loidl, A.; Hermetter, A. Oxidized phospholipids: from molecular properties to disease. *Biochim. Biophys. Acta* **2007**, *1772*, 718–736.
- (11) Halliwell, B.; Gutteridge, J. M. Role of free radicals and catalytic metal ions in human disease: an overview. *Methods Enzymol.* **1990**, *186*, 1–85.
- (12) Gutteridge, J. M.; Halliwell, B. Free radicals and antioxidants in the year 2000. A historical look to the future. *Ann. N.Y. Acad. Sci.* **2000**, *899*, 136–147.
- (13) Deigner, H. P.; Hermetter, A. Oxidized phospholipids: emerging lipid mediators in pathophysiology. *Curr. Opin. Lipidol.* **2008**, *19*, 289–294.
- (14) Everse, J.; Coates, P. W. Role of peroxidases in Parkinson disease: a hypothesis. *Free Radic. Biol. Med.* **2005**, *38*, 1296–1310.
- (15) Butterfield, D. A.; Drake, J.; Pocernich, C.; Castegna, A. Evidence of oxidative damage in Alzheimer's disease brain: central role for amyloid beta-peptide. *Trends Mol. Med.* **2001**, *7*, 548–554.
- (16) Dexter, D. T.; Carter, C. J.; Wells, F. R.; Javoy-Agid, F.; Agid, Y.; Lees, A.; Jenner, P.; Marsden, C. D. Basal lipid peroxidation in substantia nigra is increased in Parkinson's disease. *J. Neurochem.* **1989**, *52*, 381–389.
- (17) Bieschke, J.; Zhang, Q.; Powers, E. T.; Lerner, R. A.; Kelly, J. W. Oxidative metabolites accelerate Alzheimer's amyloidogenesis by a two-step mechanism, eliminating the requirement for nucleation. *Biochemistry* **2005**, *44*, 4977–4983.
- (18) Gorbenko, G. P.; Kinnunen, P. K. J. The role of lipid-protein interactions in amyloid-type protein fibril formation. *Chem. Phys. Lipids* **2006**, *141*, 72–82.
- (19) Markesbery, W. R. Oxidative stress hypothesis in Alzheimer's disease. *Free Radic. Biol. Med.* **1997**, *23*, 134–147.
- (20) Mark, R. J.; Pang, Z.; Geddes, J. W.; Uchida, K.; Mattson, M. P. Amyloid beta-peptide impairs glucose transport in hippocampal and cortical neurons: involvement of membrane lipid peroxidation. *J. Neurosci.* **1997**, *17*, 1046–1054.
- (21) Mark, R. J.; Lovell, M. A.; Markesbery, W. R.; Uchida, K.; Mattson, M. P. A role for 4-hydroxynonenal, an aldehydic product of lipid peroxidation, in disruption of ion homeostasis and neuronal death induced by amyloid beta-peptide. *J. Neurochem.* **1997**, *68*, 255–264.
- (22) Wood, L. G.; Gibson, P. G.; Garg, M. L. Biomarkers of lipid peroxidation, airway inflammation and asthma. *Eur. Respir. J.* **2003**, *21*, 177–186.
- (23) Diaz, M. N.; Frei, B.; Vita, J. A.; Keaney, J. F., Jr. Antioxidants and atherosclerotic heart disease. *N. Engl. J. Med.* **1997**, *337*, 408–416.
- (24) Berliner, J. A.; Heinecke, J. W. The role of oxidized lipoproteins in atherogenesis. *Free Radic. Biol. Med.* **1996**, *20*, 707–727.
- (25) Zhang, X. Y.; Tan, Y. L.; Cao, L. Y.; Wu, G. Y.; Xu, Q.; Shen, Y.; Zhou, D. F. Antioxidant enzymes and lipid peroxidation in different forms of schizophrenia treated with typical and atypical antipsychotics. *Schizophr. Res.* **2006**, *81*, 291–300.
- (26) Stark, G. The effect of ionizing radiation on lipid membranes. *Biochim. Biophys. Acta* **1991**, *1071*, 103–122.
- (27) Porter, N. A.; Caldwell, S. E.; Mills, K. A. Mechanisms of free radical oxidation of unsaturated lipids. *Lipids* **1995**, *30*, 277–290.
- (28) Wong-Ekkabut, J.; Xu, Z. T.; Triampo, W.; Tang, I. M.; Tieleman, D. P.; Monticelli, L. Effect of lipid peroxidation on the properties of lipid bilayers: A molecular dynamics study. *Biophys. J.* **2007**, *93*, 4225–4236.
- (29) Khandelia, H.; Mouritsen, O. G. Lipid gymnastics: evidence of complete acyl chain reversal in oxidized phospholipids from molecular simulations. *Biophys. J.* **2009**, *96*, 2734–2743.
- (30) Johnstone, S. R.; Ross, J.; Rizzo, M. J.; Straub, A. C.; Lampe, P. D.; Leitinger, N.; Isakson, B. E. Oxidized phospholipid species promote in vivo differential cx43 phosphorylation and vascular smooth muscle cell proliferation. *Am. J. Pathol.* **2009**, *175*, 916–924.
- (31) Plochberger, B.; Stockner, T.; Chiantia, S.; Brameshuber, M.; Weghuber, J.; Hermetter, A.; Schwiller, P.; Schutz, G. J. Cholesterol slows down the lateral mobility of an oxidized phospholipid in a supported lipid bilayer. *Langmuir* **2010**, *26*, 17322–17329.
- (32) Beranova, L.; Cwiklik, L.; Jurkiewicz, P.; Hof, M.; Jungwirth, P. Oxidation changes physical properties of phospholipid bilayers: fluorescence spectroscopy and molecular simulations. *Langmuir* **2010**, *26*, 6140–6144.
- (33) Mattila, J. P.; Sabatini, K.; Kinnunen, P. K. Interaction of cytochrome c with 1-palmitoyl-2-azelaoyl-sn-glycero-3-phosphocholine: evidence for acyl chain reversal. *Langmuir* **2008**, *24*, 4157–4160.
- (34) Conte, E.; Megli, F. M.; Khandelia, H.; Jeschke, G.; Bordignon, E. Lipid peroxidation and water penetration in lipid bilayers: A W-band EPR study. *Biochim. Biophys. Acta* **2013**, *1828*, 510–517.
- (35) Lis, M.; Wizert, A.; Przybylo, M.; Langner, M.; Swiatek, J.; Jungwirth, P.; Cwiklik, L. The effect of lipid oxidation on the water permeability of phospholipids bilayers. *Phys. Chem. Chem. Phys.* **2011**, *13*, 17555–17563.
- (36) Cwiklik, L.; Jungwirth, P. Massive oxidation of phospholipid membranes leads to pore creation and bilayer disintegration. *Chem. Phys. Lett.* **2010**, *486*, 99–103.
- (37) Volinsky, R.; Cwiklik, L.; Jurkiewicz, P.; Hof, M.; Jungwirth, P.; Kinnunen, P. K. Oxidized phosphatidylcholines facilitate phospholipid flip-flop in liposomes. *Biophys. J.* **2011**, *101*, 1376–1384.
- (38) Bockmann, R. A.; Hac, A.; Heimbürg, T.; Grubmüller, H. Effect of sodium chloride on a lipid bilayer. *Biophys. J.* **2003**, *85*, 1647–1655.
- (39) Garcia-Manyes, S.; Oncins, G.; Sanz, F. Effect of ion-binding and chemical phospholipid structure on the nanomechanics of lipid bilayers studied by force spectroscopy. *Biophys. J.* **2005**, *89*, 1812–1826.
- (40) Garcia-Manyes, S.; Oncins, G.; Sanz, F. Effect of pH and ionic strength on phospholipid nanomechanics and on deposition process onto hydrophilic surfaces measured by AFM. *Electrochim. Acta* **2006**, *51*, 5029–5036.
- (41) Fukuma, T.; Higgins, M. J.; Jarvis, S. P. Direct imaging of lipid-ion network formation under physiological conditions by frequency modulation atomic force microscopy. *Phys. Rev. Lett.* **2007**, *98*, 106101.
- (42) Fukuma, T.; Higgins, M. J.; Jarvis, S. P. Direct imaging of individual intrinsic hydration layers on lipid bilayers at Angstrom resolution. *Biophys. J.* **2007**, *92*, 3603–3609.
- (43) Bockmann, R. A.; Grubmüller, H. Multistep binding of divalent cations to phospholipid bilayers: a molecular dynamics study. *Angew. Chem., Int. Ed. Engl.* **2004**, *43*, 1021–1024.
- (44) Pandit, S. A.; Bostick, D.; Berkowitz, M. L. Molecular dynamics simulation of a dipalmitoylphosphatidylcholine bilayer with NaCl. *Biophys. J.* **2003**, *84*, 3743–3750.
- (45) Gurtovenko, A. A.; Miettinen, M.; Karttunen, M.; Vattulainen, I. Effect of monovalent salt on cationic lipid membranes as revealed by molecular dynamics simulations. *J. Phys. Chem. B* **2005**, *109*, 21126–21134.
- (46) Sachs, J. N.; Nanda, H.; Petrache, H. I.; Woolf, T. B. Changes in phosphatidylcholine headgroup tilt and water order induced by monovalent salts: molecular dynamics simulations. *Biophys. J.* **2004**, *86*, 3772–3782.
- (47) Miettinen, M. S.; Gurtovenko, A. A.; Vattulainen, I.; Karttunen, M. Ion dynamics in cationic lipid bilayer systems in saline solutions. *J. Phys. Chem. B* **2009**, *113*, 9226–9234.
- (48) Gurtovenko, A. A.; Vattulainen, I. Effect of NaCl and KCl on phosphatidylcholine and phosphatidylethanolamine lipid membranes: Insight from atomic-scale simulations for understanding salt-induced effects in the plasma membrane. *J. Phys. Chem. B* **2008**, *112*, 1953–1962.
- (49) Straatsma, T. P.; Berendsen, H. J. C. Free energy of ionic hydration: Analysis of a thermodynamic integration technique to

evaluate free energy differences by molecular dynamics simulations. *J. Chem. Phys.* **1988**, *89*, 5876–5886.

(50) Lindahl, E.; Hess, B.; van der Spoel, D. GROMACS 3.0: a package for molecular simulation and trajectory analysis. *J. Mol. Model.* **2001**, *7*, 306–317.

(51) Beglov, D.; Roux, B. Finite representation of an infinite bulk system: Solvent boundary potential for computer simulations. *J. Chem. Phys.* **1994**, *100*, 9050–9063.

(52) Shinoda, K.; Shinoda, W.; Mikami, M. Molecular dynamics simulation of an archaeal lipid bilayer with sodium chloride. *Phys. Chem. Chem. Phys.* **2007**, *9*, 643–650.

(53) Filippov, A.; Oradd, G.; Lindblom, G. Effect of NaCl and CaCl₂ on the lateral diffusion of zwitterionic and anionic lipids in bilayers. *Chem. Phys. Lipids* **2009**, *159*, 81–87.

(54) Ferber, U. M.; Kaggwa, G.; Jarvis, S. P. Direct imaging of salt effects on lipid bilayer ordering at sub-molecular resolution. *Eur. Biophys. J.* **2011**, *40*, 329–338.

(55) Porter, N. A.; Wujek, D. G. Autoxidation of Polyunsaturated Fatty Acids, an Expanded Mechanistic Study. *J. Am. Chem. Soc.* **1984**, *106*, 2626–2629.

(56) Berendsen, H. J. C.; Postma, J. P. M.; van Gunsteren, W. F.; Hermans, J. In *Intermolecular Forces*, Pullman, B., Ed.; D. Reidel: Dordrecht, The Netherlands, 1981; pp 331–342.

(57) Hess, B.; Holm, C.; Van Der Vegt, N. Osmotic coefficients of atomistic NaCl (aq) force fields. *J. Chem. Phys.* **2006**, *124*, 164509.

(58) Hess, B.; Kutzner, C.; van der Spoel, D.; Lindahl, E. GROMACS 4: Algorithms for highly efficient, load-balanced, and scalable molecular simulation. *J. Chem. Theory Comput.* **2008**, *4*, 435–447.

(59) Darden, T.; York, D.; Pedersen, L. Particle Mesh Ewald - an N·Log(N) Method for Ewald Sums in Large Systems. *J. Chem. Phys.* **1993**, *98*, 10089–10092.

(60) Essmann, U.; Perera, L.; Berkowitz, M. L.; Darden, T.; Lee, H.; Pedersen, L. G. A Smooth Particle Mesh Ewald Method. *J. Chem. Phys.* **1995**, *103*, 8577–8593.

(61) Karttunen, M.; Rottler, J.; Vattulainen, I.; Sagui, C. Electrostatics in biomolecular simulations: Where are we now and where are we heading? *Curr. Top. Membr.* **2008**, *60*, 49–89.

(62) Wong-ekkabut, J.; Karttunen, M. Assessment of Common Simulation Protocols for Simulations of Nanopores, Membrane Proteins, and Channels. *J. Chem. Theory Comput.* **2012**, *8*, 2905–2911.

(63) Patra, M.; Karttunen, M.; Hyvonen, M. T.; Falck, E.; Lindqvist, P.; Vattulainen, I. Molecular dynamics simulations of lipid bilayers: major artifacts due to truncating electrostatic interactions. *Biophys. J.* **2003**, *84*, 3636–3645.

(64) Patra, M.; Karttunen, M.; Hyvonen, M. T.; Falck, E.; Vattulainen, I. Lipid bilayers driven to a wrong lane in molecular dynamics simulations by subtle changes in long-range electrostatic interactions. *J. Phys. Chem. B* **2004**, *108*, 4485–4494.

(65) Hess, B.; Bekker, H.; Berendsen, H. J. C.; Fraaije, J. G. E. M. LINCS: A linear constraint solver for molecular simulations. *J. Comput. Chem.* **1997**, *18*, 1463–1472.

(66) Berendsen, H. J. C.; Postma, J. P. M.; Vangunsteren, W. F.; Dinola, A.; Haak, J. R. Molecular-Dynamics with Coupling to an External Bath. *J. Chem. Phys.* **1984**, *81*, 3684–3690.

(67) Humphrey, W.; Dalke, A.; Schulten, K. VMD: visual molecular dynamics. *J. Mol. Graph.* **1996**, *14*, 33–38.

(68) Mason, R. P.; Walter, M. F.; Mason, P. E. Effect of oxidative stress on membrane structure: small-angle X-ray diffraction analysis. *Free Radic. Biol. Med.* **1997**, *23*, 419–425.

(69) Lee, S. J.; Song, Y.; Baker, N. A. Molecular dynamics simulations of asymmetric NaCl and KCl solutions separated by phosphatidylcholine bilayers: Potential drops and structural changes induced by strong Na⁺-lipid interactions and finite size effects. *Biophys. J.* **2008**, *94*, 3565–3576.

(70) Valley, C. C.; Perlmutter, J. D.; Braun, A. R.; Sachs, J. N. NaCl Interactions with Phosphatidylcholine Bilayers Do Not Alter Membrane Structure but Induce Long-Range Ordering of Ions and Water. *J. Membr. Biol.* **2011**, *244*, 35–42.

(71) Rodriguez, J. R.; Garcia, A. E. Concentration dependence of NaCl ion distributions around DPPC lipid bilayers. *Interdiscip. Sci.* **2011**, *3*, 272–282.

(72) Petrache, H. I.; Dodd, S. W.; Brown, M. F. Area per lipid and acyl length distributions in fluid phosphatidylcholines determined by (2)H NMR spectroscopy. *Biophys. J.* **2000**, *79*, 3172–3192.

(73) Vermeer, L. S.; de Groot, B. L.; Reat, V.; Milon, A.; Czaplicki, J. Acyl chain order parameter profiles in phospholipid bilayers: computation from molecular dynamics simulations and comparison with 2H NMR experiments. *Eur. Biophys. J.* **2007**, *36*, 919–931.

(74) Chiu, S.-W.; Clark, M.; Balaji, S.; Subramaniam, S.; Scott, H. L.; Jakobsson, E. Incorporation of surface tension into molecular dynamics simulation of an interface: A fluid phase lipid bilayer membrane. *Biophys. J.* **1995**, *69*, 1230–1245.

(75) Gurtovenko, A. A.; Patra, M.; Karttunen, M.; Vattulainen, I. Cationic DMPC/DMTAP lipid bilayers: Molecular dynamics study. *Biophys. J.* **2004**, *86*, 3461–3472.

(76) Wohler, J.; Edholm, O. Dynamics in atomistic simulations of phospholipid membranes: Nuclear magnetic resonance relaxation rates and lateral diffusion. *J. Chem. Phys.* **2006**, *125*, 204703–204710.

(77) Falck, E.; Rog, T.; Karttunen, M.; Vattulainen, I. Lateral diffusion in lipid membranes through collective flows. *J. Am. Chem. Soc.* **2008**, *130*, 44–45.

(78) Konig, S.; Pfeiffer, W.; Bayerl, T.; Richter, D.; Sackmann, E. Molecular dynamics of lipid bilayers studied by incoherent quasi-elastic neutron scattering. *J. Phys. II Fr.* **1992**, *2*, 1589–1615.

(79) Tabony, J.; Perly, B. Quasielastic neutron scattering measurements of fast local translational diffusion of lipid molecules in phospholipid bilayers. *Biochim. Biophys. Acta* **1990**, *1063*, 67–72.

(80) Busch, S.; Smuda, C.; Pardo, L. C.; Unruh, T. Molecular mechanism of long-range diffusion in phospholipid membranes studied by quasielastic neutron scattering. *J. Am. Chem. Soc.* **2010**, *132*, 3232–3233.

(81) Falck, E.; Patra, M.; Karttunen, M.; Hyvonen, M. T.; Vattulainen, I. Lessons of slicing membranes: Interplay of packing, free area, and lateral diffusion in phospholipid/cholesterol bilayers. *Biophys. J.* **2004**, *87*, 1076–1091.

(82) Edholm, O.; Johansson, J. Lipid bilayer polypeptide interactions studied by molecular dynamics simulation. *Eur. Biophys. J.* **1987**, *14*, 203–209.